# Deep Learning for Accelerometric Data Assessment and Ataxic Gait Monitoring

Aleš Procházka, *Life Member, IEEE*, Ondřej Dostál, Pavel Cejnar, Hagar Ibrahim Mohamed, Zbyšek Pavelek, Martin Vališ, and Oldřich Vyšata, *Member, IEEE*

***Abstract*— Ataxic gait monitoring and assessment of neurological disorders belong to important multidisciplinary areas that are supported by digital signal processing methods and machine learning tools. This paper presents the possibility of using accelerometric data to optimise deep learning convolutional neural network systems to distinguish between ataxic and normal gait. The experimental dataset includes 860 signal segments of 16 ataxic patients and 19 individuals from the control set with the mean age of 38.6 and 39.6 years, respectively. The proposed methodology is based upon the analysis of frequency components of accelerometric signals simultaneously recorded at specific body positions with a sampling frequency of 60 Hz. The deep learning system uses all of the frequency components in a range of ⟨0, 30⟩ Hz. Our classification results are compared with those obtained by standard methods, which include the support vector machine, Bayesian methods, and the two-layer neural network with features estimated as the relative power in selected frequency bands. Our results show that the appropriate selection of sensor positions can increase the accuracy from 81.2% for the foot position to 91.7% for the spine position. Combining the input data and the deep learning methodology with five layers increased the accuracy to 95.8%. Our methodology suggests that artificial intelligence methods and deep learning are efficient methods in the assessment of motion disorders and they have a wide range of further applications.**

***Index Terms*— Accelerometric signal analysis, computational intelligence, deep learning, classification, motion monitoring.**

Manuscript received October 8, 2020; revised December 9, 2020; accepted January 9, 2021. Date of publication January 12, 2021; date of current version March 2, 2021. This work was supported in part by the Ministry of Health of the Czech Republic under Grant FN HK 00179906, in part by the Charles University, Prague, Czech Republic, under Grant PROGRES Q40, in part by the Project PERSONMED–Centre for the Development of Personalized Medicine in Age-Related Diseases, under Grant CZ.02.1.01-0.0-0.0-17_048-0007441, in part by the European Regional Development Fund (ERDF), in part by the Governmental Budget of the Czech Republic, under Grant INTER-ACTION LTAIN19007, and in part by the Development of Advanced Computational Algorithms for Evaluating Post-Surgery Rehabilitation as well under Grant LTAIN19007. *(Corresponding author: Aleš Procházka.)*

Aleš Procházka and Pavel Cejnar are with the Department of Computing and Control Engineering, University of Chemistry and Technology, 166 28 Prague, Czech Republic, and also with the Czech Institute of Informatics, Robotics and Cybernetics, Czech Technical University, 166 36 Prague, Czech Republic (e-mail: a.prochazka@ieee.org).

Ondřej Dostál, Hagar Ibrahim Mohamed, Zbyšek Pavelek, Martin Vališ, and Oldřich Vyšata are with the Department of Neurology, Faculty of Medicine in Hradec Králové, Charles University, 500 05 Hradec Králové, Czech Republic.

Digital Object Identifier 10.1109/TNSRE.2021.3051093

## I. Introduction

GAIT assessment and the study of motion disorders [1]–[5] have a wide range of applications in early diagnostics in neurology [6]–[8], physical therapy, rehabilitation, and physical activity analysis. The ataxic gait monitoring of patients with the multiple sclerosis forms a very important problem in this area. The recent rapid progress of sensor technology and wireless communication links allow the use of different microelectromechanical sensor units (MEMS), video, depth and thermal camera systems [9], [10], and wearable devices [11]–[15] for the associated motion analysis [16]–[19]. Specific mathematical methods are then used to process data in the time, frequency, or scale domains to perform human activity analysis.

This paper is devoted to the analysis of the gait patterns [20] that are related to ataxia [12], [21]–[24] as a neurological disorder associated with the loss of balance [6], [25]. The present analysis is based on three-axis accelerometric data of 16 ataxic patients and 19 healthy controls. All of the datasets were acquired by a system of sensors located at different positions [8] of the body, using a full-body motion capture device (Perception Neuron [26]) to simultaneously record accelerometric data [27] during the gait. Figure 1 presents an example of some possible locations for accelerometers used for data acquisition.

Computational intelligence and standard classification methods, including decision tree (DT), $k$-nearest neighbour (k-NN), support vector machines (SVM), Bayesian methods, and the two-layer neural network (NN) algorithms, are often used in this area [28]. All these methods assume the appropriate selection of features in the time, frequency and scale [29] domains.

Another more complex approach is based on the use of artificial intelligence and deep neural networks (DNNs) [30]–[35] that are applied to optimize multilayer mathematical systems and their coefficients. These methods are often used in the analysis of the body's motion [36], for the natural kinematics of human activity recognition [37]–[40], and for the evaluation of motion disorders. They allow us to avoid many of the problems related to feature selection and they are also used for more effective decision making in some cases. Although this complex approach [41], [42] to the construction of classification models can be very efficient, it needs sophisticated software and powerful computational tools.

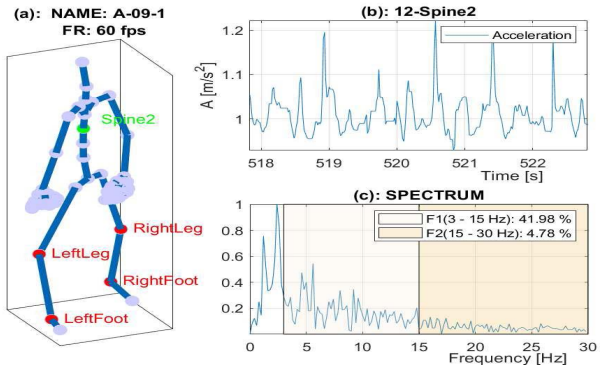


Fig. 1. Principle of data processing presenting (a) accelerometric data acquisition using a wearable sensor in the chosen (spine) area of the body, (b) the time segment of the data module 5 s long, and (c) associated spectral values in the range of $\langle 0, f_S/2\rangle$ Hz for the sampling frequency $f_S = 60$ Hz used as patterns for the deep learning or for the estimation of features as the mean power in selected frequency ranges.

The goal of the present study is to contribute to the analysis of accelerometric data for motion monitoring and to compare the results of the deep learning with further classification methods for the recognition of different motion patterns associated with an ataxic gait. From the more general point of view, it contributes to the classification of motion disorders in neurology. It also allows us to improve the treatment outcomes and to reduce the need for invasive procedures. the results point to the use of artificial intelligence methods in human activity monitoring and motion analysis in different areas.

## II. Methods

### A. Data Acquisition

Accelerometric signals recorded during the gait allow the detection of motion patterns that are important for recognition of movement disorders. Figure 1 presents the principle of simultaneous data acquisition by the Perception neuron system [8], [26], [43] that uses 31 sensor units located at different parts of the body. This system enables the simultaneous recording of accelerometric data at different body positions with a given sampling frequency. Subjects wearing this device were asked to walk forth and back in the 20 m long hospital corridor (with the smooth floor surface) according to their individual physical capabilities but with the maximum walk length limited to 500 m. Records were split into 5 s long segments including straight gait and turns. Poor quality parts (in case of sensor detachment or gait interruption) were manually removed.

The statistics of all 35 individuals who participated at this study are summarized in Table I, which includes facts about two separate classes and a total number of $Q = 860$ segments:

1) Class CA - norm: the control set of 19 individuals (355 time windows 5 s long),
2) Class CB - ataxic patients with the diagnosis of multiple sclerosis: 16 individuals (505 time windows 5 s long).

The diagnosis of these individuals was evaluated by two experienced neurologists according to their behaviour during the gait. The project was approved by the Local Ethics Committee in accordance with the 1964 Helsinki declaration.

TABLE I
Statistics of Experiments Including the Number of Individuals, Their Mean Age and Standard Deviation (STD), and Number of Segments Belonging to Class CA (Norm) and CB (Ataxia)

| *Class* | *Number* | *Age [Years]* | | *Segments* |
|---|---|---|---|---|
| | | *Mean* | *STD* | |
| CA - *norm* | 19 | 39.6 | 9.7 | 355 |
| CB - *ataxia* | 16 | 38.6 | 16.1 | 505 |
| *SUM:* | 35 | | | 860 |

Simultaneous recording of accelerometric data with a sampling frequency of $f_s = 60$ Hz was performed by the perception neuron after its initial calibration. Each time frame included accelerometric data in three directions for specific body positions. Their modulus was then used for data analysis.

All of the data segments of accelerometric signals related to both classes were randomly divided into the training and testing sets with 90% and 10% of observations, respectively. The selection was done randomly but with a balanced number of segments belonging to classes CA and CB. A comparison of classification accuracies was then evaluated for both the training and testing sets.

Figure 2(a) presents spectral values of signals that belong to class CA (norm) and class CB (ataxic diagnosis) with their mean values. Figures 2(b,c) present the training and testing sets that we used to classify and validate the results, respectively.

### B. Feature Extraction and Classification

Data processing included statistical analysis of individual accelerometric records for each class (class CA: control set, class CB: ataxic gait) recorded with a sampling frequency $f_s = 60$ Hz. Accelerometric signal sets $T = 5$ s long were recorded in three directions $\{[s_x(n), s_y(n), s_z(n)]\}_{n=0}^{N-1}$ and then used to evaluate their modulus $\{x(n)\}_{n=0}^{N-1}$ for $N = T\ f_s$ samples. Each record was then transformed by the discrete Fourier transform (DFT) into the frequency domain, which was used to separate the signals into individual classes.

The signal features can be evaluated in both the time and transform domains using either the discrete Fourier or wavelet transforms [44]. In these domains, the time dependent features can be evaluated and spectrograms or scalograms can be used to optimise the structure and coefficients of complex mathematical models for data classification. Our proposed approach uses the simple discrete Fourier transform (DFT) of each time segment $\{x(n)\}_{n=0}^{N-1}$ $N$ samples long, forming the sequence $\{X(k)\}_{k=0}^{N-1}$

$$X(k) = \sum_{n=0}^{N-1} x(n)\ \exp(-j\ k\ n\ 2\ \pi/N) \tag{1}$$

for frequency values $f_k = k/N\ f_s, k = 0, 1, \cdots, N-1$ which appears to be sufficient in the given application.

The pattern matrix of $Q$ columns that will be used for the following classification was defined by the following two methods:

- Deep learning: each column of the pattern matrix included $N/2$ values of each spectral curve in the training

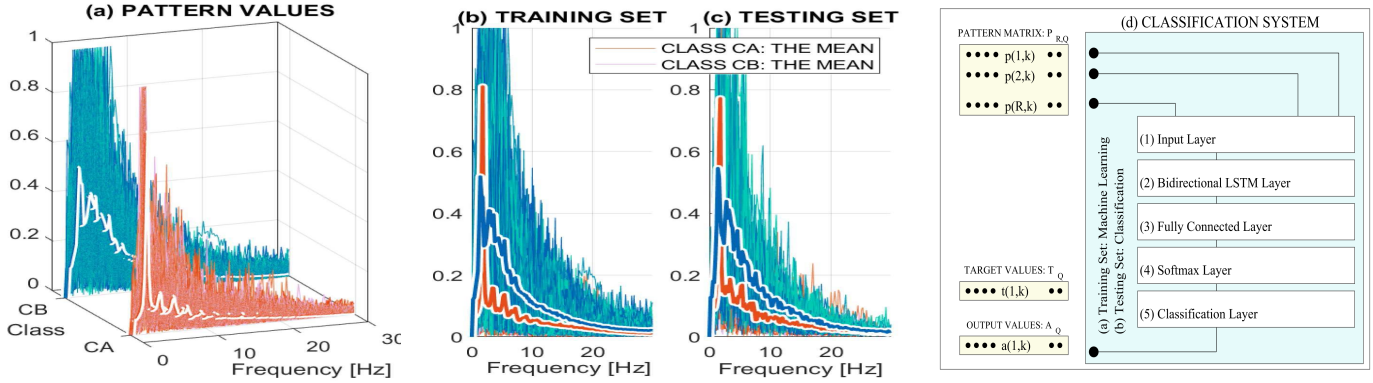


Fig. 2. Selection of pattern values from segments belonging to class CA (norm) and class CB (ataxic diagnosis) presenting (a) spectral component of individual segments and their mean values, (b) the training set, (c) the testing set randomly selected from all experiments, and (d) data processing by the deep learning classification system with five layers using column vectors of spectral components for each segment in the pattern matrix and corresponding probabilities of class belongings at the output.

set with a frequency resolution of $f_s/N$ Hz for the chosen total number of $N/2$ frequency samples $\{X(k)\}_{k=0}^{N/2-1}$.

- Standard classification methods: each column of the pattern matrix included two values of two specific features that were associated with each sample in the training set, which were estimated in the frequency domains.

Target values associated with each column of the pattern matrix were defined by an experienced neurologist in both cases (class CA-control set, class CB-ataxic gait).

The features that we used for standard classification are based upon spectral components in the frequency domain, including:

(i) The relative mean power in the range $\langle f_{a1}, f_{a2}\rangle$,
(ii) The relative mean power in the range $\langle f_{a3}, f_{a4}\rangle$.

Each of spectral features of a signal segment $\{x(n)\}_{n=0}^{N-1}$ $N$ samples long was evaluated using the discrete Fourier transform in terms of the relative power $P$ in the frequency band $\langle f_{ai}, f_{aj}\rangle$, as follows:

$$P = \frac{\sum_{k\in\Phi} |X(k)|^2}{\sum_{k=0}^{N/2} |X(k)|^2} \tag{2}$$

where $\Phi$ is the set of indices for frequencies $f_k \in \langle f_{ai}, f_{aj}\rangle$.

Figure 3 presents the distribution of selected couples of features that we used for the standard classification using the relative mean power in the frequency range of $\langle 15, 30\rangle$ Hz versus the relative mean power in the frequency range of $\langle 3, 15\rangle$ Hz with centers and $c$-multiples of standard deviations of each class for $c = 0.2, c = 0.5$ and $c = 1$. The feature clusters that are presented in Fig. 3(a) for the spine2 location of the accelerometric sensor are much better separated then those obtained from data recorded by accelerometers at the right foot position that are presented in Fig. 3(b), which corresponds with the study [8].

## C. Movement Recognition

Pattern values in the feature matrix $\mathbf{P}_{R,Q}$ and the associated target vector $\mathbf{T}_{1,Q}$ were used to classify all of the $Q$ feature vectors or signal segments into separate categories

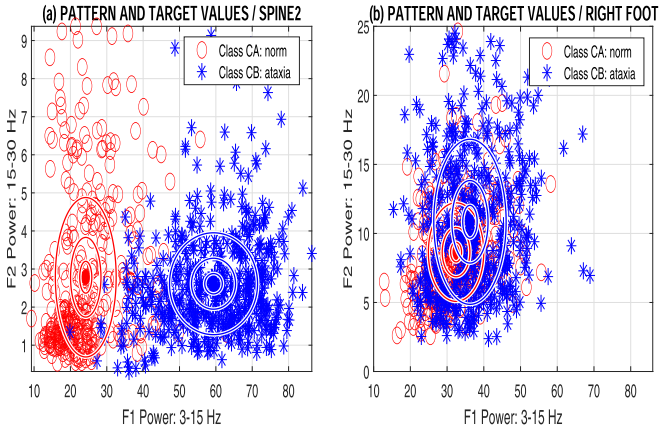


Fig. 3. The distribution of features using the relative mean power in the frequency range of $\langle 15, 30\rangle$ Hz versus the relative mean power in the frequency range of $\langle 3, 15\rangle$ Hz with centers and $c$-multiples of standard deviations of each class for $c = 0.2$, $c = 0.5$, and $c = 1$ for (a) the spine2 position and (b) the right foot position of the accelerometric sensor.

using specific machine learning methods [45], [46]. The results of the deep learning system were then compared with those evaluated by classical systems, which included a SVM, a Bayesian method, and a two-layer NN. Both the accuracies and the cross-validation errors were then used to evaluate the individual results.

In the deep learning strategy, the classification system included the input layer with $R = N/2$ elements in the basic case, bidirectional long short term memory (LSTM) [47], fully connected layer, softmax layer and the classification layer [45], [48] as presented in Fig. 2(d). Each input vector included all $R = N/2$ values of the DFT defined by Eq. (1).

The two-layer NN system was defined by a simplified system with coefficients $\mathbf{W1}_{S1,R}$, $\mathbf{W2}_{S2,S1}$, $\mathbf{b1}_{S1,1}$, $\mathbf{b2}_{S2,1}$. Each input vector of feature matrix $\mathbf{P}_{R,Q}$ included $R = 2$ values only evaluated as the mean power in two frequency bands estimated by Eq. (2). The system evaluated output values by the following relations:

$$\mathbf{A1}_{S1,Q} = f1(\mathbf{W1}_{S1,R}\,\mathbf{P}_{R,Q}, \mathbf{b1}_{S1,1}) \tag{3}$$

$$\mathbf{A2}_{S2,Q} = f2(\mathbf{W2}_{S2,S1}\,\mathbf{A1}_{S1,Q}, \mathbf{b2}_{S2,1}) \tag{4}$$

TABLE II
THE CONFUSION MATRIX WITH RESULTS OF THE TWO-CLASS CLASSIFICATION SYSTEM FOR CLASS CA (NEGATIVE) AND CLASS CB (POSITIVE) VALUES

| *Predicted (Output) Class* \ *True (Target) Class* | Negative | Positive | Predictive Value |
|---|---|---|---|
| Negative | True Negative (**TN**) | False Negative (**FN**) | $NPV=\frac{TN}{TN+FN}$ |
| Positive | False Positive (**FP**) | True Positive (**TP**) | $PPV=\frac{TP}{TP+FP}$ |
| True Rate | $TNR=\frac{TN}{TN+FP}$ | $TPR=\frac{TP}{TP+FN}$ | |

For each column vector in the pattern matrix, the corresponding target vector specifies the associated class as defined in the learning stage.

The proposed models use the sigmoidal transfer function $f1$ in the first layer and the probabilistic softmax transfer function $f2$ in the final layer. The values of the output layer, which are based on Bayes's theorem [49], provide the probabilities of each class.

The performance of classification models is often evaluated by the log-loss function, which takes into account the probability that is assigned to the estimation of the target value. This can be evaluated by the following relation

$$LL=-\frac{1}{Q}\sum_{i=1}^{Q}(t(i)\log(p(i))+(1-t(i))\log(1-p(i))) \quad (5)$$

where $t(i)$ stands for the binary output to be predicted, $p(i)$ stands for the probability assigned by the model, and $Q$ is the number of target values. The coefficients of the classification system are then optimised during the machine learning process to minimise the value of this criterion, whose strength lies in the fact that the log-loss function combines the correct and strong prediction. In addition, as a measure of predictive inaccuracy, it should be as low as possible.

The selection of the classification model is closely related to the application area and the number of pattern values that are used for system optimisation in the learning stage. In many applications, simple classification systems provide sufficient results. However, in the case of more complicated patterns, DNNs with specific (convolutional) layers [45] are often used for effective decision making with a sufficient generalisation ability.

The receiver operating characteristic (ROC) curves were used as an efficient tool to evaluate the classification results. The selected classifier finds in the negative set (controls) and positive set (atactic gait) the number of true-negative (TN), false-positive (FP), true-positive (TP) and false-negative (FN) experiments.

The associated performance metrics [50] can then be used to evaluate:

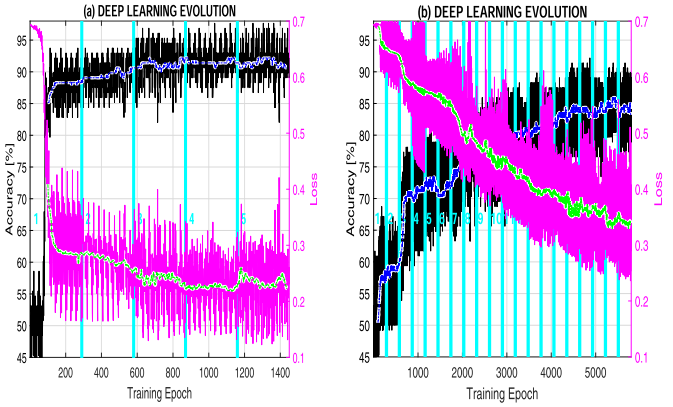


Fig. 4. The evolution of the accuracy and the loss for the norm and ataxic patients during the selected number of training epochs of the deep learning system for (a) the spine2 position of the accelerometric sensor with the final accuracy of 92.2% after 1400 learning epochs and (b) the right foot position of the accelerometric sensor with a final accuracy of 84.3% after 6000 learning epochs.

- The true positive rate (sensitivity) and the true negative rate (specificity)

$$TPR=\frac{TP}{TP+FN}, \quad TNR=\frac{TN}{TN+FP} \quad (6)$$

- The false negative rate and the false positive rate

$$FNR=\frac{FN}{TP+FN}, \quad FPR=\frac{FP}{TN+FP} \quad (7)$$

- The negative predictive value and the positive predictive value (precision)

$$NPV=\frac{TN}{TN+FN}, \quad PPV=\frac{TP}{TP+FP} \quad (8)$$

- Accuracy

$$ACC=\frac{TP+TN}{TP+TN+FP+FN} \quad (9)$$

Cross-validation errors were then evaluated as a measure of the generalization abilities of classification models using the leave-one-out method.

## III. RESULTS

The optimisation process was done for the DNN structure presented in Fig. 2(d) in the incremental mode, which allowed us to modify the structure and network coefficients during the learning stage. This process aimed to optimise the network to maximise the accuracy and to minimise the loss during individual epochs. This optimisation was performed using the mathematical and software environment of the Matlab2020b system.

Figure 4 presents the evolution of the accuracy and the loss during the selected number of incremental learning stages of the deep learning system. This process enabled us to improve the behaviour of the DNN that we used for classification with the randomly selected training system initialisations. Figure 4(a) presents results for the spine2 and Fig. 4(b) for the right foot position of the accelerometric sensor with the final accuracy of the training set 92.2% and 84.3%, respectively.

TABLE III

ACCURACY (ACC) AND THE LOSS VALUE OF CLASSIFICATION INTO TWO CLASSES BY THE DEEP LEARNING METHOD FOR DIFFERENT POSITIONS OF ACCELEROMETRIC SENSORS WITH THEIR FINAL VALUES AND THEIR MEAN OVER THE LAST FIVE LEARNING EPOCHS OF THE TRAINING STAGE

| *Accelerometer Position* | *No. Epochs* | *Accuracy [%]* | | *Loss* | |
|---|---|---|---|---|---|
| | | *Final* | *Mean5* | *Final* | *Mean5* |
| Spine2 | 1400 | 92.2 | 92.6 | 0.24 | 0.21 |
| RightFoot (RF) | 6000 | 84.3 | 83.9 | 0.34 | 0.36 |
| Spine2 & RF | 7250 | 95.8 | 96.0 | 0.09 | 0.13 |

TABLE IV

CONFUSION MATRIX OF THE CLASSIFICATION BY THE DEEP LEARNING (DL) NEURAL NETWORK MODEL FOR THE TRAINING AND TESTING SETS WITH TRUE POSITIVE VALUES ON THE MATRIX DIAGONAL (IN THE BOLD), TRUE POSITIVE/NEGATIVE RATES *TR*(*k*), AND POSITIVE/NEGATIVE PREDICTION VALUES *PV*(*k*) FOR THE SPINE2 ACCELEROMETER POSITION

*Precision Colorbar*: 55 60 65 70 75 80 85 90 95 100

*(a) DL MATRIX / Training*

| *Output* \ *Class k* | *Target* CA | *Target* CB | $PV(k)$ |
|---|---|---|---|
| CA | **281** | 38 | 88.1 |
| CB | 12 | **307** | 96.2 |
| $TR(k)$ | 95.9 | 90.0 | **ACC: 92.2** |

*(b) DL MATRIX / Testing*

| *Output* \ *Class k* | *Target* CA | *Target* CB | $PV(k)$ |
|---|---|---|---|
| CA | **32** | 4 | 88.9 |
| CB | 2 | **34** | 94.0 |
| $TR(k)$ | 94.1 | 89.5 | **ACC: 91.7** |

TABLE V

CONFUSION MATRIX OF THE CLASSIFICATION BY THE DEEP LEARNING (DL) NEURAL NETWORK MODEL FOR THE TRAINING AND TESTING SETS WITH TRUE POSITIVE VALUES ON THE MATRIX DIAGONAL (IN THE BOLD), TRUE POSITIVE/NEGATIVE RATES *TR*(*k*), AND POSITIVE/NEGATIVE PREDICTION VALUES *PV*(*k*) FOR THE RIGHT FOOT ACCELEROMETER POSITION

*Precision Colorbar*: 55 60 65 70 75 80 85 90 95 100

*(a) DL MATRIX / Training*

| *Output* \ *Class k* | *Target* CA | *Target* CB | $PV(k)$ |
|---|---|---|---|
| CA | **270** | 49 | 84.6 |
| CB | 51 | **268** | 84.0 |
| $TR(k)$ | 84.1 | 84.5 | **ACC: 84.3** |

*(b) DL MATRIX / Testing*

| *Output* \ *Class k* | *Target* CA | *Target* CB | $PV(k)$ |
|---|---|---|---|
| CA | **29** | 7 | 80.5 |
| CB | 6 | **30** | 83.3 |
| $TR(k)$ | 82.9 | 81.0 | **ACC: 81.2** |

Table III summarizes further results, which also include the loss values.

Tables IV and V present associated confusion matrices of the final deep learning model for two accelerometer positions, and for both the training and testing sets. The precision of the testing set is much better for the spine2 position (with the accuracy of 91.7%) in comparison with the right foot sensor (with the accuracy of 81.2%).

Figure 5 presents the results of the network with predicted probabilities of classes CA and CB for the input test set of signal segments that belong to class CA (norm) and class CB (ataxia) with associated classification errors for accelerometer located at the spine2 (in Figures 5(a,b)) and at the right foot (in Figures 5(c,d)).

The classification results achieved for the DNNs were compared with those evaluated by the SVM method, Bayesian

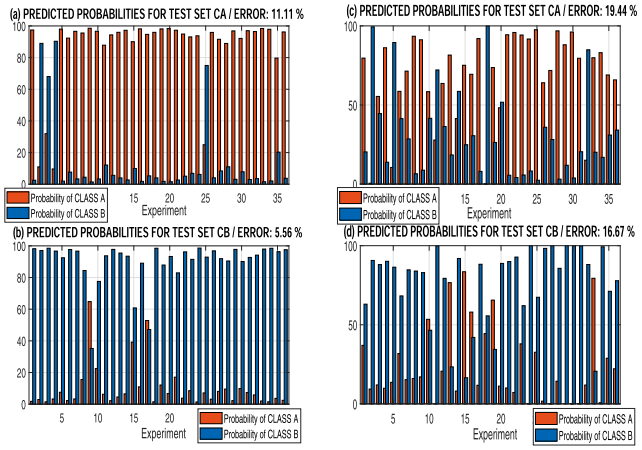


Fig. 5. Results of a network test presenting predicted probabilities of classes CA and CB for the input test set of signal segments that belong to class CA (norm) and class CB (ataxia) with associated classification errors for an accelerometer located at position (a,b) spine2 and (c,d) right foot.

TABLE VI

ACCURACY (ACC) AND CROSS-VALIDATION ERRORS (CV) FOR CLASSIFICATION OF ACCELEROMETRIC DATA INTO TWO CLASSES BY THE SVM, BAYESIAN METHOD, AND THE TWO-LAYER NN FOR THE SPINE2 AND THE RIGHT FOOT SENSOR POSITIONS

| *Method* | *Spine2* | | *Right Foot* | |
|---|---|---|---|---|
| | *ACC [%]* | *CV* | *ACC [%]* | *CV* |
| SVM Method | 89.5 | 0.056 | 65.1 | 0.349 |
| Bayes' Method | 87.3 | 0.069 | 63.7 | 0.363 |
| 2-layers NN | 90.7 | 0.060 | 68.6 | 0.321 |
| MEAN: | 89.2 | 0.062 | 65.8 | 0.344 |

method (Naïve Bayes' Classifier), and the two layer NN with the sigmoidal and softmax transfer functions. Table VI presents the accuracy and cross validation errors for classification of data acquired at different positions of accelerometric sensors. The results of the classification for the SVM, Bayesian method, and the two-layer NN are very close, with a mean accuracy of 89.2% and 65.8% for the spine2 and the right foot sensor position, respectively. The mean value of cross-validation of 0.062 and 0.344 for the spine2 and the right foot position, respectively, also point to completely different features of these datasets and to the importance of the appropriate selection of sensor positions to obtain reliable classification results.

Figure 6 presents the classification into two classes (class CA: control set, class CB: ataxic patients) for two features evaluated as the relative power in two frequency bands using selected classification methods with the accuracy ($AC$) and the $k$-fold cross-validation ($CV$) errors (for $k = 10$) with visualisation of class boundaries.

The deep learning system for processing of accelerometric data acquired either at the spine2 or the right foot position had $R = 150$ input elements that represented 150 spectral components evaluated for 5 s long data segments recorded with the sampling frequency of 60 Hz. To obtain more reliable results, these two records were combined into pattern vectors of $R = 300$ elements. Figure 7(a) presents results of the associated deep learning process of 7250 training epochs and 25 incremental learning stages with a final training

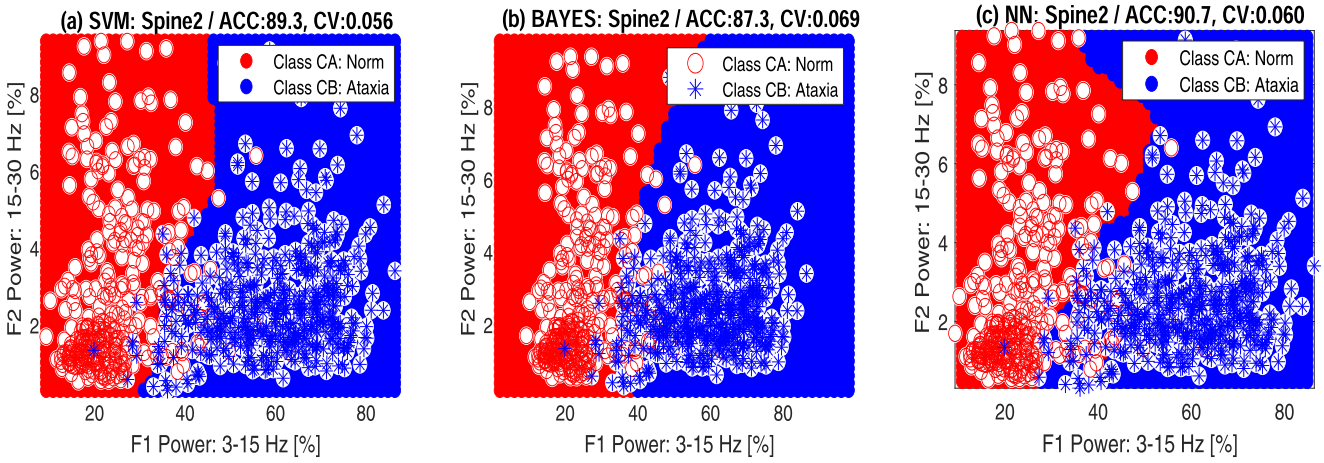


Fig. 6. Classification of accelerometric data for two features evaluated as the relative power in two frequency bands using: (a) the SVM method, (b) Bayesian method, and (c) the two layer NN with accuracy (*AC* [%]) and cross-validation (*CV*) errors.

TABLE VII
CONFUSION MATRIX OF THE CLASSIFICATION BY THE DEEP LEARNING (DL) NEURAL NETWORK MODEL FOR THE TRAINING AND TESTING SETS WITH TRUE POSITIVE VALUES ON THE MATRIX DIAGONAL (IN THE BOLD), TRUE POSITIVE/NEGATIVE RATES *TR*(*k*), AND POSITIVE/NEGATIVE PREDICTION VALUES *PV*(*k*) FOR THE SPINE2 AND THE RIGHT FOOT POSITIONS OF THE ACCELEROMETRIC SENSOR

*Precision Colorbar*

| 55 | 60 | 65 | 70 | 75 | 80 | 85 | 90 | 95 | 100 |
|---|---|---|---|---|---|---|---|---|---|

*(a) DL MATRIX / Training*

| *Output* \ *Class* *k* | *Target* CA | *Target* CB | $PV(k)$ |
|---|---|---|---|
| CA | **304** | 15 | 95.3 |
| CB | 12 | **307** | 96.2 |
| $TR(k)$ | 96.2 | 95.3 | **ACC: 95.8** |

*(b) DL MATRIX / Testing*

| *Output* \ *Class* *k* | *Target* CA | *Target* CB | $PV(k)$ |
|---|---|---|---|
| CA | **34** | 2 | 94.4 |
| CB | 1 | **35** | 97.2 |
| $TR(k)$ | 97.1 | 94.6 | **ACC: 95.8** |

accuracy and loss of 95.8% and 0.09, respectively. The more complex structure of input elements required additional computational time but the accuracy and the loss was better than for a single accelerometer only, as compared in Table III.

Table VII presents the associated confusion matrices of the final neural network model for this complex model based upon datasets from different sensors. The precision is higher than 94.4% in all cases.

Figures 7(b,c) present the predicted probabilities of classes CA and CB for the input test set of signal segments that belong to class CA (norm) and class CB (ataxia) with associated classification errors. The total number of three segments out of 72 from the testing set was misclassified. It is assumed that this number can be decreased further with the use of additional sensors, even though the learning process will be longer. The advantage of deep learning is that it is not necessary to specify any signal features in advance, which is compensated by very extensive datasets and complex model structures.

## IV. DISCUSSION

The results of the accelerometric data analysis correspond with those published recently [6], [51], [52] and they point to the possibility to use upper-body movements as a clinical biomarker during the gait. These suggestions are based on

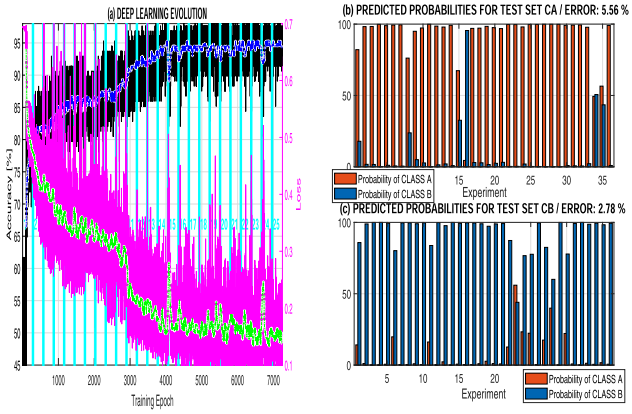


Fig. 7. Results of the deep learning for the spine2 and the right foot position of the accelerometric sensor presenting (a) the evolution of the accuracy and the loss for the norm and ataxic patients during 25 incremental learning stages and 7250 training epochs with the final accuracy and loss 95.8% and 0.09, respectively; and the network test presenting predicted probabilities of (b) classes CA and (c) class CB for the input test set of signal segments that belong to class CA (norm) and class CB (ataxia) with associated classification errors.

the fact that ankle sensors record less involuntary movements owing to their partial stabilization by the contact with the floor. Sensors placed in the upper part of the body are therefore more sensitive to separation of normal and ataxic gait. The classification accuracy for sensors located on the left/right foot of about 77% increased to more than 98% for sensors located on the head, spine or shoulders [8]. These results allow the replacement of the complex set of accelerometric sensors by the one wearable sensor in the selected position only.

Accelerometric data processing forms a complementary approach to traditional gait analysis that use stepping characteristics [49], [53] to discriminate ataxic patients from controls. Moreover, its accuracy is higher than that of different models based on the selection of spatial domain features [54], [55] with an accuracy between 70 and 80% in the early stage of the disease [53], [56].

Ataxic gait monitoring and analysis is based upon reliable data acquisition and their processing. The paper shows that

accelerometric signals can be used to distinguish gait disorders as an alternative to observation by camera systems. Data processing is then related to deep learning and to construction of feature vectors by complete signal segments transformed into the frequency domain. This approach with no specification of features enables the simplification of the whole classification process and sufficient accuracy in many applications.

## V. Conclusion

This paper has presented the use of selected mathematical methods for the classification of accelerometric data recorded for 35 individuals of the similar age with normal or ataxic gate. The whole database included 860 signal segments, each of them was 5 seconds long and they were recorded with a sampling frequency of 60 Hz. Both standard and deep learning methods were used to distinguish gait features and to select patients with neurological disorders.

Standard classification tools included the SVM, Bayesian method and the two layer NN. The mean accuracy was 89.2% and 65.8% for accelerometric data recorded at the spine2 and the right foot position, respectively. The results obtained by the complex multilayer neural network optimized by the deep learning method provided a classification accuracy of 95.8%.

It was confirmed that accelerometric data and their mathematical processing in the frequency domain can be used to classify signal segments into two categories, which represent normal or ataxic gait. The present research has also confirmed that the selection of appropriate positions of sensors is very important for reliable classification and better separation abilities of motion patterns. In addition it was verified that classification of motion patterns by accelerometers is affected by two main factors: (i) optimal positioning of accelerometric sensors, and (ii) appropriate selection of computational tools and associated mathematical methodology.

The advantages of the deep learning system are that no selection of features was necessary and that better classification of segments was achieved. The advantage of standard methods was in better possibilities for visualization, simpler models, and faster optimization of its coefficients. Therefore, a combination of both approaches to data processing can lead to a deeper understanding of the physical behaviour of the studied system.

This paper forms a multidisciplinary approach to neurological data processing with the use of computational intelligence to contribute to the more reliable diagnostics of neurological disorders. It describes how wearable sensors and appropriate data processing tools can be useful in the detection of motion patterns and their analysis.

Our future work will be devoted to the verification of these results using more extensive datasets. We will also further study appropriate sensor positions in relation to different neurological problems and specific motion patterns. In addition, deep learning methods will be applied to datasets preprocessed by further functional transforms. Thanks to the complicated structures and incremental learning strategy of deep learning systems, it will be possible to study changes in the system structure and its coefficients during the learning process.

The general background of our research suggests that it may be possible to use motion patterns classification in many different areas using similar mathematical tools. For example, feature-based methods can benefit from the visual assessment of their distribution. Meanwhile, deep learning methods can be used for the direct analysis of observed sequences, either in the time or frequency domains, without any initial selection of features but with specific demands for a much more complex computational environment. In both cases, new machine learning strategies, and their implementation for neurological data processing and physical activity monitoring will be studied.

Further research will be devoted to gait analysis by different sensors using accelerometers, gyrometers, and video based systems [19], [49], [57] as well. Depth sensors and RGB cameras are based upon processing of video sequences acquired in the limited spatial area. Wearable sensors have no such limits but their accuracy is affected by many additional signal components. It seems that multivariable data processing, including studies of simultaneously recorded EEG signals, and their time synchronized processing can also contribute to better diagnosis of neurological disorders in the clinical environment.

## References


[1] A. Mannini, S. S. Intille, M. Rosenberger, A. M. Sabatini, and W. Haskell, "Activity recognition using a single accelerometer placed at the wrist or ankle," *Med. Sci. Sports Exerc.*, vol. 45, no. 11, pp. 2193–2203, Nov. 2013.

[2] K. Konsolakis, "Physical activity recognition using wearable accelerometers in controlled and free-living environments," M.S. thesis, Dept. Biomed. Signals Syst., TU Delft, Delft, The Netherlands, 2018.

[3] N. Twomey *et al.*, "A comprehensive study of activity recognition using accelerometers," *Informatics*, vol. 5, no. 2, pp. 5:1–5:37, May 2018.

[4] S. Mehrang *et al.*, "Human activity recognition using a single optical heart rate monitoring wristband equipped with triaxial accelerometer," in *Proc. EMBEC, NBC*, H. Eskola, O. Väisänen, J. Viik, and J. Hyttinen, Eds. Singapore: Springer, 2018, pp. 587–590.

[5] A. Mannini and S. S. Intille, "Classifier personalization for activity recognition using wrist accelerometers," *IEEE J. Biomed. Health Inform.*, vol. 23, no. 4, pp. 1585–1594, Jul. 2019.

[6] E. Buckley, C. Mazzà, and A. McNeill, "A systematic review of the gait characteristics associated with cerebellar ataxia," *Gait Posture*, vol. 60, pp. 154–163, Feb. 2018.

[7] D. Arvidsson, J. Fridolfsson, and M. Börjesson, "Measurement of physical activity in clinical practice using accelerometers," *J. Internal Med.*, vol. 286, no. 2, pp. 137–153, Apr. 2019.

[8] O. Dostál, A. Procházka, O. Vyšata, O. Ťupa, P. Cejnar, and M. Vališ, "Recognition of motion patterns using accelerometers for ataxic gait assessment," *Neural Comput. Appl.*, vol. 32, pp. 1–9, Jun. 2020.

[9] M. M. Hassan, M. Z. Uddin, A. Mohamed, and A. Almogren, "A robust human activity recognition system using smartphone sensors and deep learning," *Future Gener. Comput. Syst.*, vol. 81, pp. 307–313, Apr. 2018.

[10] A. Hickey, S. D. Din, L. Rochester, and A. Godfrey, "Detecting free-living steps and walking bouts: Validating an algorithm for macro gait analysis," *Physiol. Meas.*, vol. 38, no. 1, pp. N1–N15, Jan. 2017.

[11] S. Sanei, D. Jarchi, and A. Constantinides, *Body Sensor Networking, Design and Algorithms*. Hoboken, NJ, USA: Wiley, 2020.

[12] D. Jarchi, J. Pope, T. K. M. Lee, L. Tamjidi, A. Mirzaei, and S. Sanei, "A review on accelerometry-based gait analysis and emerging clinical applications," *IEEE Rev. Biomed. Eng.*, vol. 11, pp. 177–194, 2018.

[13] C. Charalambous and A. Bharath, "A data augmentation methodology for training machine/deep learning gait recognition algorithms," in *Proc. Brit. Mach. Vis. Conf. (BMVA)*, 2016, pp. 110:1–110:12.

[14] A. H. K. Montoye, J. M. Pivarnik, L. M. Mudd, S. Biswas, and K. A. Pfeiffer, "Comparison of activity type classification accuracy from accelerometers worn on the hip, wrists, and thigh in young, apparently healthy adults," *Meas. Phys. Educ. Exerc. Sci.*, vol. 20, no. 3, pp. 173–183, Jul. 2016.

[15] J. Wang, Y. Chen, S. Hao, X. Peng, and L. Hu, "Deep learning for sensor-based activity recognition: A survey," *Pattern Recognit. Lett.*, vol. 119, pp. 3–11, Mar. 2019.

[16] A. Procházka, S. Vaseghi, H. Charvátová, O. Ťupa, and O. Vyšata, "Cycling segments multimodal analysis and classification using neural networks," *Appl. Sci.*, vol. 7, no. 6, pp. 581:1–581:11, Jun. 2017.

[17] H. Charvátová, A. Procházka, S. Vaseghi, O. Vyšata, and M. Vališ, "GPS-based analysis of physical activities using positioning and heart rate cycling data," *Signal, Image Video Process.*, vol. 11, no. 2, pp. 251–258, Feb. 2017.

[18] A. Procházka, H. Charvátová, S. Vaseghi, and O. Vyšata, "Machine learning in rehabilitation assessment for thermal and heart rate data processing," *IEEE Trans. Neural Syst. Rehabil. Eng.*, vol. 26, no. 6, pp. 1209–1214, Jun. 2018.

[19] A. Procházka, O. Vyšata, H. Charvátová, and M. Vališ, "Motion symmetry evaluation using accelerometers and energy distribution," *Symmetry*, vol. 11, no. 7, pp. 2929:1–2929:13, 2019.

[20] M. Serrao and C. Conte, "Detecting and measuring ataxia in gait," in *Handbook Human Motion*, B. Müller and S. Wolf, Eds. Cham, Switzerland: Springer, 2018, pp. 937–954.

[21] A. D'Ambrosio *et al.*, "Cerebellar contribution to motor and cognitive performance in multiple sclerosis: An MRI sub-regional volumetric analysis," *Multiple Sclerosis J.*, vol. 23, no. 9, pp. 1194–1203, Aug. 2017.

[22] P. Chen, Y. Kuang, and J. Li, "Human motion capture algorithm based on inertial sensors," *J. Sensors*, vol. 2016, pp. 4343797:1–4343797:15, Jan. 2016.

[23] G. Grimaldi and M. Manto, "Neurological tremor: Sensors, signal processing and emerging applications," *Sensors*, vol. 10, no. 2, pp. 1399–1422, Feb. 2010.

[24] B. Kashyap, D. Phan, P. N. Pathirana, M. Horne, L. Power, and D. Szmulewicz, "Objective assessment of cerebellar ataxia: A comprehensive and refined approach," *Sci. Rep.*, vol. 10, no. 1, pp. 9493:1–9493:17, Dec. 2020.

[25] H. Stolze, "Typical features of cerebellar ataxic gait," *J. Neurol., Neurosurg. Psychiatry*, vol. 73, no. 3, pp. 310–312, Sep. 2002.

[26] H. Kim *et al.*, "Application of a perception neuron system in simulation-based surgical training," *J. Clin. Med.*, vol. 8, no. 1, pp. 124:1–124:14, Jan. 2019.

[27] D. Álvarez, J. Alvarez, R. González, and A. López, "Upper limb joint angle measurement in occupational health," *Comput. Methods Biomech. Biomed. Eng.*, vol. 19, no. 2, pp. 1–12, 2015.

[28] A. Procházka, J. Kuchyňka, O. Vyšata, P. Cejnar, M. Vališ, and V. Mařík, "Multi-class sleep stage analysis and adaptive pattern recognition," *Appl. Sci.*, vol. 8, no. 5, pp. 697:1–697:14, May 2018.

[29] E. Hošťálkova, O. Vyšata, and A. Procházka, "Multi-dimensional biomedical image de-noising using Haar transform," in *Proc. 15th Int. Conf. Digit. Signal Process.*, Cardiff, U.K., Jul. 2007, pp. 175–179.

[30] C. Cao *et al.*, "Deep learning and its applications in biomedicine," *Genomics, Proteomics Bioinf.*, vol. 16, no. 1, pp. 17–32, Feb. 2018.

[31] A. Raza, A. Mehmood, S. Ullah, M. Ahmad, G. S. Choi, and B.-W. On, "Heartbeat sound signal classification using deep learning," *Sensors*, vol. 19, no. 21, pp. 4819:1–4819:15, Nov. 2019.

[32] H. Nishizaki and K. Makino, "Signal classification using deep learning," in *Proc. IEEE Int. Conf. Sensors Nanotechnol.*, Penang, Malaysia, Jul. 2019, pp. 1–4.

[33] A. Sangaiah, *Deep Learning and Parallel Computing Environment for Bioengineering Systems*. Amsterdam, The Netherlands: Elsevier, 2019.

[34] H. I. Fawaz, G. Forestier, J. Weber, L. Idoumghar, and P.-A. Müller, "Deep learning for time series classification: A review," *Data Mining Knowl. Discovery*, vol. 33, no. 4, pp. 917–963, Jul. 2019.

[35] B. Almaslukh, A. Artoli, and J. Al-Muhtadi, "A robust deep learning approach for position-independent smartphone-based human activity recognition," *Sensors*, vol. 18, no. 11, p. 3726, Nov. 2018.

[36] Y. Gu, Z. Shao, L. Qin, W. Lu, and M. Li, "A deep learning framework for cycling maneuvers classification," *IEEE Access*, vol. 7, pp. 28799–28809, 2019.

[37] N. Neverova *et al.*, "Learning human identity from motion patterns," *IEEE Access*, vol. 4, pp. 1810–1820, 2016.

[38] N. Golestani and M. Moghaddam, "Human activity recognition using magnetic induction-based motion signals and deep recurrent neural networks," *Nature Commun.*, vol. 11, no. 1, pp. 1551:1–1551:11, Dec. 2020.

[39] K. Wang and W. Zhou, "Pedestrian and cyclist detection based on deep neural network fast R-CNN," *Int. J. Adv. Robot. Syst.*, vol. 16, no. 2, pp. 1–10, 2019.

[40] L. Sadouk and T. Gadi, "Convolutional neural networks for human activity recognition in time and frequency-domain," *Adv. Intell. Sys. Comput.*, vol. 756, pp. 485–496, Jan. 2019.

[41] I. Goodfellow, Y. Bengio, and A. Courville, *Deep Learning*. Cambridge, MA, USA: MIT Press, 2016.

[42] A. Antoniades *et al.*, "Detection of interictal discharges with convolutional neural networks using discrete ordered multichannel intracranial EEG," *IEEE Trans. Neural Syst. Rehabil. Eng.*, vol. 25, no. 12, pp. 2285–2294, Dec. 2017.

[43] T. Baumann, T. Hao, Y. He, and R. Shoda, *Perception Neuron Unity Handbook*, 27th ed. Beijing, China: Noitom Technology, 2017.

[44] E. Jerhotová, J. Švihlík, and A. Procházka, *Biomedical Image Volumes Denoising Via the Wavelet Transform*. London, U.K.: INTECH, 2011, pp. 435–458.

[45] I. Goodfellow, Y. Bengio, and A. Courville, *Deep Learning*. Cambridge, MA, USA: MIT Press, 2016.

[46] K. He, X. Zhang, S. Ren, and J. Sun, "Deep residual learning for image recognition," in *Proc. IEEE Conf. Comput. Vis. Pattern Recognit.*, Jun. 2016, pp. 770–778.

[47] F. Ordóñez and D. Roggen, "Deep convolutional and LSTM recurrent neural networks for multimodal wearable activity recognition," *Sensors*, vol. 16, no. 1, pp. 115:1–115:25, Jan. 2016.

[48] M. Nielsen, *Neural Networks and Deep Learning*. Washington, DC, USA: Determination Press, 2015.

[49] A. Procházka, O. Vyšata, M. Vališ, O. Ťupa, M. Schatz, and V. Mařík, "Bayesian classification and analysis of gait disorders using image and depth sensors of microsoft Kinect," *Digit. Signal Process.*, vol. 47, pp. 169–177, Dec. 2015.

[50] A. Procházka, O. Vyšata, O. Ťupa, M. Yadollahi, and M. Vališ, "Discrimination of axonal neuropathy using sensitivity and specificity statistical measures," *Neural Comput. Appl.*, vol. 25, no. 6, pp. 1349–1358, Nov. 2014.

[51] R. Krishna, P. N. Pathirana, M. Horne, L. Power, and D. J. Szmulewicz, "Quantitative assessment of cerebellar ataxia, through automated limb functional tests," *J. Neuroeng. Rehabil.*, vol. 16, no. 1, pp. 31:1–31:15, Dec. 2019.

[52] D. Phan, N. Nguyen, P. N. Pathirana, M. Horne, L. Power, and D. Szmulewicz, "Quantitative assessment of ataxic gait using inertial sensing at different walking speeds," in *Proc. 41st Annu. Int. Conf. IEEE Eng. Med. Biol. Soc. (EMBC)*, Jul. 2019, pp. 4600–4603.

[53] C. Buckley *et al.*, "The role of movement analysis in diagnosing and monitoring neurodegenerative conditions: Insights from gait and postural control," *Brain Sci.*, vol. 9, no. 2, pp. 34:1–34:21, Feb. 2019.

[54] T. A. Zilani, F. Al-Turjman, M. B. Khan, N. Zhao, and X. Yang, "Monitoring movements of ataxia patient by using UWB technology," *Sensors*, vol. 20, no. 3, pp. 931:1–931:16, Feb. 2020.

[55] A. López, F. Ferrero, and O. Postolache, "An affordable method for evaluation of ataxic disorders based on electrooculography," *Sensors*, vol. 19, no. 17, pp. 3756:1–3756:16, Aug. 2019.

[56] G. Rizzo, M. Copetti, S. Arcuti, D. Martino, A. Fontana, and G. Logroscino, "Accuracy of clinical diagnosis of Parkinson disease: A systematic review and meta-analysis," *Neurology*, vol. 86, no. 6, pp. 566–576, 2016.

[57] A. Prochazka, M. Schatz, O. Tupa, M. Yadollahi, O. Vysata, and M. Walls, "The MS Kinect image and depth sensors use for gait features detection," in *Proc. IEEE Int. Conf. Image Process. (ICIP)*, Oct. 2014, pp. 2271–2274.